8th IAA Planetary Defense Conference – PDC 2023
3-7 April 2023, Vienna, Austria

IAA-PDC-23-01-47
CHARACTERIZATION OF NEAR-EARTH OBJECTS USING PLANETARY RADAR OBSERVATIONS AND NUMERICAL MODELING

Anne Virkki(1)(2)
(1)*University of Helsinki, Gustaf Hällströmin katu 2, 00560 Helsinki, anne.virkki@helsinki.fi*
(2)*Finnish Geospatial Research Institute, National Land Survey, Vuorimiehentie 5, Espoo*

Keywords: *Asteroids, Near-Earth Objects, Radar, Physical characterization*

Extended Abstract

Introduction

Planetary radar observations provide a powerful tool for the post-discovery characterisation of the physical and dynamical properties of asteroids, comets, the Moon, and terrestrial planets. I will present recent results of radar observations of near-Earth asteroids observed at the Arecibo Observatory [1], which have increased our understanding of the diversity of potentially hazardous asteroids in terms of sizes, shapes, binarity, and composition. These characteristics are crucial to planetary defense as they play a role in the selection of the optimal mitigation technique. Planetary radar systems can measure the asteroid's radar cross section in two opposite or orthogonal polarization states and the Doppler broadening, which provide information on the asteroid's size, rotation rate, and the composition. They can also be used for range-Doppler imaging by mapping the reflected power as a function of the Doppler frequency and the range (based on the signal's round-trip time), which allows imaging resolutions finer than 10 meters at best, and thus direct observations of morphologic features and possible moons.

Due to the penetration depths of several wavelengths and the wide parameter space in scattering inversion problems, understanding the physical characteristics of near-Earth objects (NEOs) based on their radar scattering profiles requires extensive numerical modeling. Traditionally, circular polarization ratio has been used as a first-order gauge to the surface roughness, but more recent advances in numerical modeling demonstrate that better measures exist (e.g., [2-3]), which can help us to understand better the physical characteristics of NEOs. One improvement is to evaluate the radar albedos of each polarization separately, which allows the reflectivity information to remain. This has been commonly done for the opposite-circular (OC) polarization but not the same-circular (SC) polarization component (w.r.t. the transmitted radar signal). As shown in [2], plotting the OC radar albedo against SC radar albedo instead of the SC/OC ratio can reveal for example boulder abundance more easily. A further improvement is evaluating each component as a function of incidence angle (a disk function) if the image resolution allows. This allows distinguishing different scattering processes (quasi-specular versus diffuse scattering), which is crucial to evaluate the size-frequency distribution of the regolith. For example, the disk function of 101955 Bennu shows no specular component, which indicates that wavelength-scale particles dominate the surface. For contrast, the Moon has a strong quasi-specular spike, which is consistent with the fact that fine-grained regolith dominates the lunar surface.

Radar scattering laws have been traditionally based on modeling the backscattering coefficient as a function of incident angle derived analytically for mathematically convenient surface morphologies or empirically to match the data without proper understanding of the meaning of the empirical fit parameters. The analytically derived models assume that the surface is composed primarily of fine-grained regolith or a solid surface that forms a gently undulating interface with few or no wavelength-scale scatterers. This assumption has been reasonable for the surfaces of the terrestrial planets and moons but is not sufficient for asteroids that have often a "rubble-pile structure" and, as such, the asteroid surfaces have often a significantly greater coverage of centimeter-to-decimeter scale regolith than planets or moons. Electromagnetic scattering by a densely packed medium of wavelength-scale particles requires different modeling methods than scattering by undulating surfaces to be able to correctly model both observed polarizations. Scattering models based on an undulating surface often fail at modeling the SC polarization component.

Methods

The radar scattering processes in asteroids include two components: The fine-grained regolith can be treated as a volume with an effective electric permittivity, where the radar signal propagates with the principles of geometric optics. In the regolith and on the surface, there are wavelength (centimeter-to-decimeter) scale scatterers embedded that cause diffuse (resonance regime) scattering and produce especially the observed SC echo power. Therefore, the scattering problem is divided geometrically in two parts: Scattering by the undulating surface and scattering by the wavelength-scale particles. The latter is first treated simply as an arbitrary scattering law before diving into the interpretations of the laws.

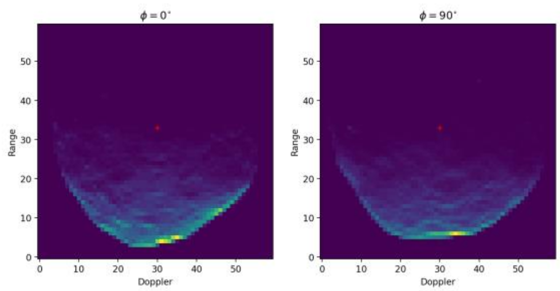

Figure 1. Synthetic radar range-Doppler images of 101955 Bennu using two rotation phases 90° apart.

We built synthetic range-Doppler images of asteroids using their shape models, if available, or ellipsoids if a shape model is not available. An example using the shape model of 101955 Bennu is shown in Fig. 1. We calculated for each triangle its range and Doppler-frequency dimension coordinates and its echo power contribution to each pixel in a range-Doppler map based on the incidence angle at each point. The direction of the incident wave can be freely selected, e.g., to match the geometry during the observation. The frequency dimension is not restricted on the rotation period but can be scale freely. The echo power contribution was calculated using a predetermined scattering law. We have using so far commonly used scattering laws such as the cosine law often used in the SHAPE software for shape modeling of asteroids: $d\sigma/dA = R\ C \cos^{2C}\theta$, where R and C are the fitting parameters so that R is the Fresnel reflectivity at the normal incidence for a plane interface and C^{-1} is the square of the root-mean-square (r.m.s.) slope (this interpretation is correct to a precision of 3 standard deviations for r.m.s. slopes up to 17° or C > 9 based on our preliminary tests for both parameters). We may then integrate the echo power of each element to find the total radar cross section and the radar albedo in addition to the disk function (backscattering coefficient as a function of incidence angle or range). Figure 2 illustrates the method applied to the shape model of Bennu. R and C parameters derived using SHAPE are 0.56 and 0.078, respectively (M.C. Nolan, personal communication). We were able to reproduce the radar cross section and radar albedo using these values together with the Bennu shape model, which validates the credibility of the code. These values were for the OC polarization, but if radar albedos in each polarization are needed, we can use two separate sets of scattering parameters.

The synthetic radar images can be used for a variety of purposes. By adding noise, we can investigate how the addition of the noise affects the certainty of the asteroid's size when estimated from the radar image. This can be done for different shape models to also evaluate the role of the shape on the size uncertainty. Another benefit is deriving the R parameter for shape models obtained using SHAPE. During the shape-modeling process, the R parameter is typically fixed to a guessed value, and in some cases adjusted later using the continuous-wave echo power spectra. However, this step, and consequently its reporting in the resulting publication is sometimes omitted. Once the radar cross section and radar albedo have been calculated for the model, the observed radar cross section can be used for calibrating the reflectivity, i.e., the R parameter, and to estimate its uncertainty due to the orientation, noise, etc. The R parameter can be further used for estimating the electric permittivity: $\varepsilon = [(1 + \sqrt{R})/(1 - \sqrt{R})]^2$. Several equations have been proposed for deriving the near-surface density (ρ) of the target using the electric permittivity, for example Garvin et al. [4] derived $\rho = 1.77(\varepsilon^{1/2} - 1)$ to estimate the near-surface density of Venus. Hickson et al. [5] proposed $\rho = 3.26(\varepsilon^{1/3} - 1)$ based on Looyenga-Landau-Lifshitz formula and laboratory measurements of regolith analogs. Shepard et al. [6] suggested a density measure based on the radar albedo (p_{rad}): $\rho = 6.944 p_{rad} + 1.083$ when $p_{rad} > 0.07$. Using R parameters collected from publications presenting radar-data-based shape models, this method appears promising in producing densities that fall within the range of 1-6 g cm^{-3} that has been estimated based on meteorite studies.

As the second part of the work, we used our former computations of the scattering properties of laboratory-characterized particles [2, 7] to investigate the reflectivity of the particles in each polarization and the SC/OC ratio as a function of size parameter ($x=2\pi r/\lambda$, where r is the effective radius and λ is the wavelength). This approach provides clues to why the SC/OC ratios of highly porous asteroids such as Bennu do not produce high values despite the very rough surface (see Fig. 3). Here A is the most rounded particle, B and C are compact but moderately elongated, and D is flat and highly elongated (see [2] and [7] for details). B and C are the most comparable to the particles seen in images of Bennu and other spacecraft-visited asteroids. We selected two significantly different electric permittivities to compare the results to each other and to our former work of polarization properties of cluster of spherical particles at backscattering [8].

Discussion

In terms of planetary defense, the density of asteroids is a crucial component in the impact hazard of a potential impactor. Although radar scattering only provides the near-surface density, which can be different from the total bulk density, it can be indicative of the composition of the asteroid. This work also helps to estimate better the uncertainty of the size estimate using range-Doppler images without a lengthy shape-modeling process. For example, the low values of the scattering-law parameters for Bennu are as one would expect for a highly porous, rough-surfaced object. Depending on the permittivity-to-near-surface-density equation we select, we find a near-surface density of 1.4-1.9 g cm^{-3}, while the total mean density of Bennu is 1.19 ± 0.01 g cm^{-3} [9]. The near-surface density that is 20-60 % greater than the mean density is contrary to what is observed for example on the Moon. One possibility is that movement of the surface material, which is known to be much more common on Bennu than the Moon, could result in higher packing density.

The value of the scattering-law fit parameter C is much lower than the reliability limit of interpreting C as r.m.s. slope. This means that the diffuse scattering dominates, and the surface is dominated by wavelength-scale particles or other structures with radii of curvature in the wavelength scale.

The second part of the work (see results in Fig. 3) shows the role of the electric properties of the particles on asteroid surfaces on the radar properties. The selected values show strikingly clearly the difference due to the particles' electric properties as well as their shapes. Particles B and C are the most comparable shapes to particles observable in spacecraft images of surfaces such as those of Bennu, Ryugu, and Dimorphos. We find that particles with a low electric permittivity (here, 2.04) have to be significantly larger than particles with electric permittivities of 6.45 to produce comparable SC radar albedos and SC/OC ratios. Considering that the size-frequency distribution of regolith typically follows a power-law distribution with a power index of 2-4, the scattering properties of the particles with size parameters 1-5 for high-permittivity materials and 2-10 for low permittivities dominate those of the larger particles and the particles with $x<<1$ as shown in [7]. This fact highlights the role of the regolith permittivity in the observed scattering properties.

Summary and future work

Although the empirical scattering laws have been proved sufficient for the purposes of describing the overall radar-scattering profiles of planets and moons, there is a significant amount of work required for the physical characterization of asteroid near-surfaces using radar and optical data. Radar scattering laws for the diverse asteroid surfaces have not been well established. Also, understanding the role of complex-shaped particles in radar scattering is work in progress. The goal is to improve the reliability of the NEO characterization using the radar data and to help inform the optimal deflection technique development if a truly hazardous asteroid was discovered. As the preliminary work has shown, this would allow us to find the near-surface density and regolith size-frequency distributions of centimeter-to-decimeter scale particles and to improve the size estimation using radar images.

References

[1] Virkki, A. K. et al. (2022), Arecibo planetary radar observations of near-Earth asteroids: 2017 December – 2019 December, Planetary Science Journal 3, 222

[2] Virkki, A. K. & Bhiravarasu, S. S. (2019), Modeling Radar Albedos of Laboratory-Characterized Particles: Application to the Lunar Surface, Journal of Geophysical Research: Planets, Volume 124, 11

[3] Hickson, D. C., et al. (2021), Polarimetric decomposition of near-Earth asteroids using Arecibo radar observations, Planetary Science Journal 2, 30

[4] Garvin, J.B., et al. (1985), Venus global radar reflectivity and correlations with elevation, Journal of Geophysical Research 90, 6859

[5] Hickson, D.C., et al. (2018), Near surface bulk density estimates of NEAs from radar observations and permittivity measurements of powdered geologic material, Icarus 306, 16

[6] Shepard, M. K., et al. (2010), A radar survey of M- and X-class asteroids II. Summary and synthesis, Icarus 208, 221

[7] Virkki, A. & Muinonen, K. (2016), Radar scattering by planetary surfaces modelled with laboratory-characterized particles, Icarus, 269, 38

[8] Virkki, A., et al. (2012), Circular Polarization of Spherical-Particle Aggregates at Backscattering, JQSRT, 126, 150

[9] Daly et al. (2020), Hemispherical Differences in the Shape and Topography of Asteroid (101955) Bennu, Science Advances 6, eabd3649

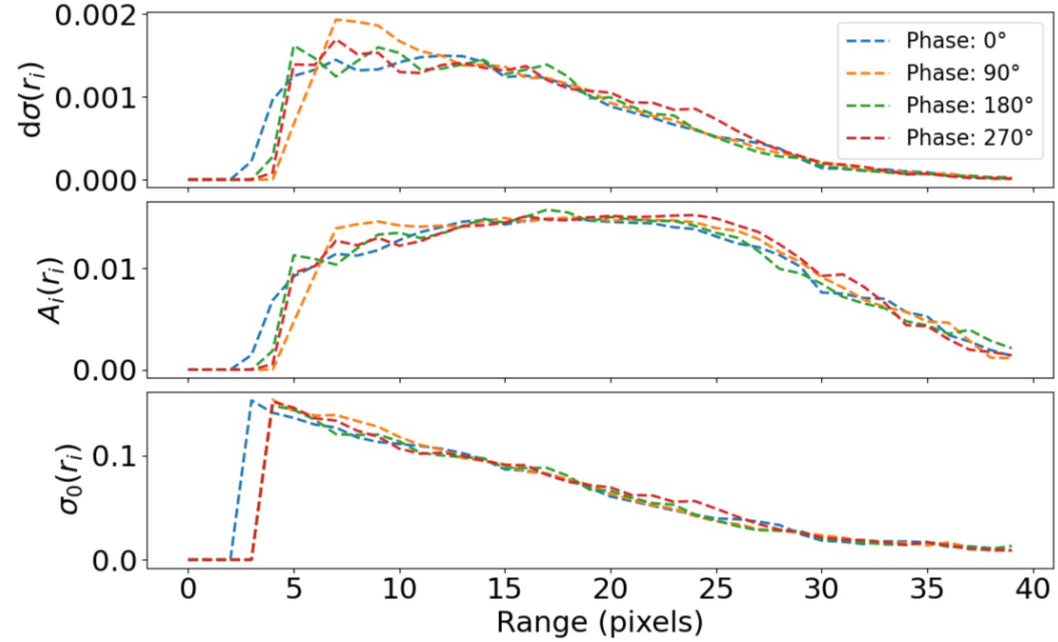

Figure 2. Integrated backscattering coefficient (on the top), integrated area (in the middle), and the area-normalized differential backscattering coefficient (on the bottom) as a function of range for a synthetic range-Doppler image using the shape model of Bennu in four different rotation phases (in equatorial view) and the cosine law with parameters R=0.056 and C=0.078 derived using SHAPE (M. Nolan, personal communication).

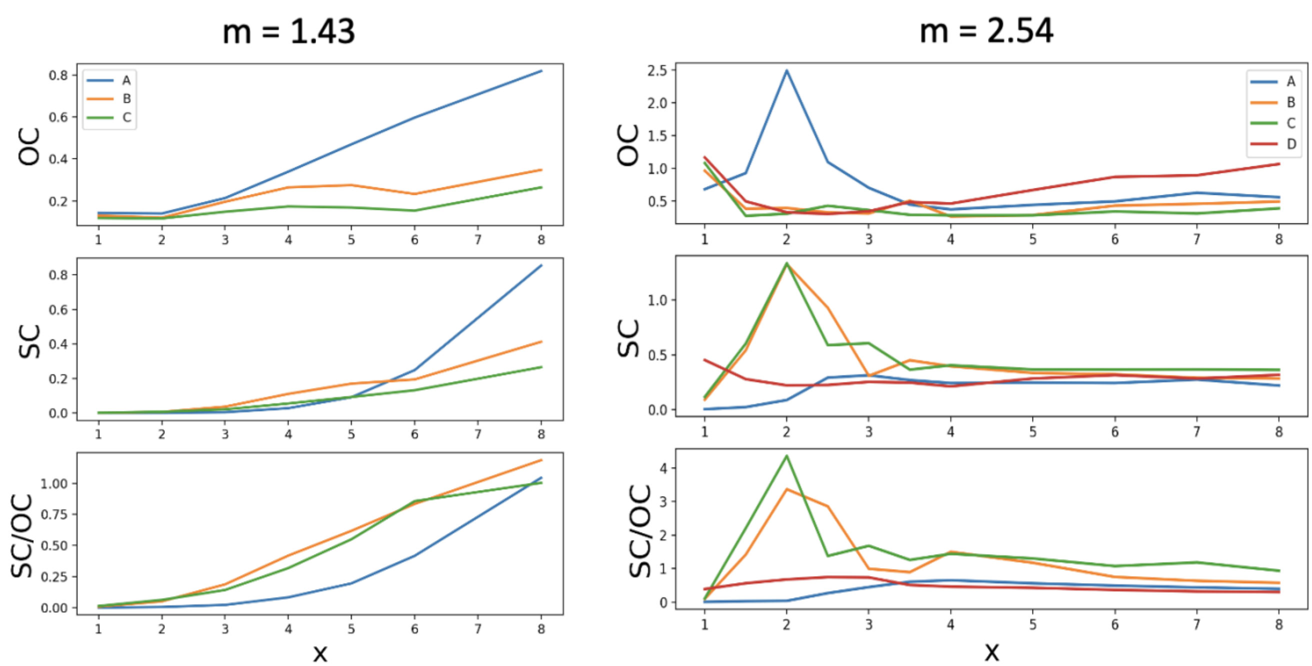

Figure 3. Radar scattering properties (OC radar albedo, SC radar albedo, and SC/OC ratio) of laboratory-characterized particles presented in [2] and [7] as a function of size parameter using two different refractive indices: on the left, m = 1.43 (ε = 2.04), and on the right, m=2.54 (ε = 6.45).